REPORT DOCUMENTATION PAGE

Form Approved
OMB No. 0704-0188

1. AGENCY USE ONLY (Leave blank)	2. REPORT DATE	3. REPORT TYPE AND DATES COVERED
	16 Apr 96	Translation

4. TITLE AND SUBTITLE
Gas-Dynamic Investigations in a Shock Tube using a Highly Sensitive Interferometer

5. FUNDING NUMBERS
AFOSR Grant
F49620-94-1-0067

6. AUTHOR(S)
Author: G. Smeets and A. George, I.S.L., France.
Translated by Andreas Goetz, Purdue University

7. PERFORMING ORGANIZATION NAME(S) AND ADDRESS(ES)
Aerospace Sciences Lab.
3 Purdue University Airport
West Lafayette IN 47906-3371

8. PERFORMING ORGANIZATION REPORT NUMBER

9. SPONSORING / MONITORING AGENCY NAME(S) AND ADDRESS(ES)
Air Force Office of Scientific Research
110 Duncan Avenue
Bolling AFB
Washington DC 20332-0001

10. SPONSORING / MONITORING AGENCY REPORT NUMBER

11. SUPPLEMENTARY NOTES
Translation of Report 14/71, Institute Franco-Allemand de Recherches de Saint-Louis, Dr. G. Smeets, June 1971. Translated by Mr. Andreas Goetz at Purdue University, School of Aeronautics and Astronautics, October 1995. Translation was corrected by G. Smeets.

12a. DISTRIBUTION / AVAILABILITY STATEMENT
Unclassified unlimited per original source document

12b. DISTRIBUTION CODE

13. ABSTRACT *(Maximum 200 words)*
The laser-interferometer described in the technical report ISL T 21/70 underwent development. Utilizing a 15 mW He-Ne laser at 6328 angstroms, and a PIN photodiode as a detector, optical path changes can now be measured with an uncertainty of 0.1 angstroms and a resolution in time of about 20 ns. Various experiments on shock tube arrangements were conducted to demonstrate the wide range of applicability and the advantages of this technique.

14. SUBJECT TERMS	15. NUMBER OF PAGES
Laser interferometer, gas dynamics	35 pages
	16. PRICE CODE

17. SECURITY CLASSIFICATION OF REPORT	18. SECURITY CLASSIFICATION OF THIS PAGE	19. SECURITY CLASSIFICATION OF ABSTRACT	20. LIMITATION OF ABSTRACT
UNCLASSIFIED	UNCLASSIFIED	UNCLASSIFIED	UL

Dr. G. Smeets - A. George
Deutsch-Französisches Forschungsinstitut Saint-Louis

Institut Franco-Allemand de Recherches de Saint-Louis
5 Rue Du General Cassagnov
68301 Saint-Louis
FRANCE

Report
14/71

Gas-Dynamic Investigations in a Shock Tube using a Highly Sensitive Interferometer

Saint-Louis
June 14, 1971

Chief Engineer
(Auriol)

Chairman at the BWB
(Dr. Schall)

Translated from German by

Andreas R. Goetz
School of
Aeronautics & Astronautics
Purdue University
West Lafayette, IN 47906, USA

W. Lafayette, Oct. 22, 1995

Abstract

The laser-interferometer described in the technical report ISL T 21/70 underwent further development. Utilizing a 15 mW (λ = 6328 Å) He-Ne laser and a PIN photo diode as a detector, optical path changes can now be measured with an uncertainty of 0.1 Å and a resolution in time of about 20 ns. Various experiments on shock tube arrangements were conducted to demonstrate the wide range of applicability and the advantages of this technique.

Contents

Introduction

The technical report ISL T 21/70 described a highly sensitive laser-interferometer set-up using Wollaston prisms. This paper reports about the subsequent development and about a number of measurements conducted with the shock tubes of the HAG[1].

Visualization of a low density flow field using interferograms is not possible, if the optical path changes are much smaller than the wavelength of the light and cause no perceptible shifts in the interference pattern. Now, instead of a film, a small photo diode with a point-like sensitive surface is installed in the interferometer image plane. The interferometer is adjusted to large interference fringe spacing, such that the region between a bright and a dark interference band is located at the photo diode. A shift of the interference pattern is then registered by the diode as a change in light intensity.

Figure 1 shows the intensity I as a function of the optical path difference $\Delta\phi$. In the middle of the slope, the intensity variations ΔI are proportional to the optical path changes $\delta\phi$:

$$\frac{\Delta I}{I_0} = \pi \cdot \frac{\delta\phi}{\lambda}. \qquad (1)$$

Using a He-Ne laser yields two decisive advantages:

1) The laser beam can easily be focussed on a diameter limited only by refraction resulting in a high spatial resolution.

2) The whole light bundle can be directed to the point-like detector. Thereby a high signal-to-noise ratio is achieved enabling highly sensitive measurements. Using a 15 mW (λ = 6328 Å) He-Ne laser and a PIN photo diode resulted in a resolution limit for optical path changes of 0.1 Å and a time resolution of 20 ns.

Set-up description

Interferometers are very sensitive to vibrations. This might pose a difficult problem for the measurement method described here. This is, because the detector must be covered by the middle of the interference slope at all times. Furthermore, no additional shift of the interference pattern due to vibrations must occur during the measurement (for instance, such vibrations can occur in the ground or at the test section windows just at the moment of the shock tube firing.).

The differential interferometer used here has the advantage of a rather low sensitivity to vibrations. The set-up scheme is displayed in figure 2. By means of the telescope, the

[1] Hypersonic Aerodynamics Group.

diameter of the laser beam can be adjusted. At the same time, the ray can be focussed on its minimal diameter in the test section, limited only by diffraction. The linear polarization of the original laser beam is converted into a circular polarization by a $\lambda/4$-plate. After this, the ray is split in a Wollaston prism into two beams polarized in directions perpendicular to each other. Those two beams, after intersecting the flow field in the test section, are merged again in the following Wollaston prism. The last Wollaston prism, with its axis rotated against the axes of the rest of the prisms by 45°, splits the ray into two parts producing complementary phased signals on the two detectors. The difference of the detector signals is registered. Thus, modulations due to noise, until now present to a lesser or greater extent in all lasers, cancel out. The signal from the flow field is doubled. The lens drawn into the figure is used for imaging the flow onto the sensitive surfaces of the detectors. Due to this measure, the whole laser light reaches the detector surfaces. Furthermore, in accordance to Fermat's principle, the optical path lengths of all light rays from the test section to the detectors are equal independent of the direction of the light ray. An additional sensitivity to a normal optical path gradient $d\delta\phi / dy$ is thereby avoided. The interference filter avoids noise generation in case of a light-emitting flow.

Should disturbances be anticipated during data acquisition (this danger exists for very sensitive measurements with a duration longer than 1 ms), an arrangement depicted in figure 3 can be employed. In this case, the laser beam is split into two beams before entering the interferometer. Two interfering pairs of light rays are generated in the test section, producing two signals on separate receivers. One of the ray pairs is shielded against interaction with the flow. The differential interferometer is adjusted, such that vibrations of the set-up generate in-phase noise signals on both receivers. By subtracting the signals, modulation due to both the vibrations and the laser light fluctuations can be simultaneously suppressed.

The computation of $\delta\phi$ (starting from this value, refraction index, gas density or electron density are calculated) is carried out using equation (1). For this, the value of ΔI, directly deducable from the recorded signal, has to be divided by I_0. If the output power of the laser is constant over extended time periods, I_0 can be determined before the data acquisition run (the interferometer is adjusted to the highest and then to the smallest intensity, and the difference between those two values is computed.). If the laser output fluctuates, an additional reference recording of the laser intensity at the instant of the data acquisition will be necessary.

The technical details of the arrangements shown in figure 2 and 3 are described in greater depth in the appendix.

Gas-dynamic measurements

A series of measurements in shock tubes have been conducted with the newly developed laser-interferometer within the last year. In part, those measurements served to solve immediate problems and were as such part of the HAG research program. The other part consisted of preliminary experiments geared towards sounding out the range of applications and the capabilities of the new measurement method.

Figure 4 shows an arrangement, by which the density of a free flow has been measured. A small tube of 10 mm diameter and 100 mm length, closed on both ends by small glass windows was placed sidewise into the flow. On both ends, the tube carried sharpened rings to prevent leakage of the gas from the stagnation region into the area in front of the windows. A laser beam is sent through the tube and remains unchanged along the whole tube length. The other ray intersects the undisturbed flow upstream. The signal in figure 4 shows a time variation of the flow typical for a hypersonic shock tube with diverging nozzle. The flow is steady only in the short time interval after the end of the starting phenomena in the nozzle and before the arrival of the driver gas puts an ends to the data acquisition run.

Using the arrangement shown in figure 5, the density distribution in a shock tube with constant diameter has been measured. The measurement chamber had a square cross section of 50 x 50 mm^2. In this case, one of the laser beams could be sent through an orifice in the side wall. The signals retrieved with this arrangement can be used for investigations into relaxation (molecular vibration, dissociation, ionisation).

The density profile within a shock front could be captured by sending the laser beams through small capillaries as sketched in figure 6. Here, the optical arrangement of figure 3 has been used. The diameter of the four laser beams measured approximately 0.1 mm in the middle of the test section. They were adjusted to be exactly perpendicular to the shock tube axis. The shock tube's inner diameter was 100 mm. The lengths of the capillaries were 10 mm and 48 mm respectively, and their inner diameter was 1 mm. They were installed exactly symmetrically in the center of the shock tube. The boundary layer on the window caused no disturbances, since all 4 laser beams were influenced in the same manner. For the same reason, the effects on the ends of the capillaries cancel out. No booster amplifier was needed. The diode circuit as depicted in figure 2 and figure 3 was directly connected to a wide frequency band oscilloscope. The circuit was designed to exhibit low capacitance and resistance, such that the resolution in time turned out to be about 20 ns.

Figure 7 shows an arrangement used for measurement of the flow in front of a sphere of only 1 mm in diameter in the supersonic flow behind the shock wave. Here, the laser beams were focussed to 0.02 mm at the locus of the sphere. The sphere is moved slowly downstream by the flow. Thus, the laser beam traverses the stagnation region. The location, at which the laser beam leaves the shock wave is of particular interest. The signal

in figure 7 shows a relatively slow decline to zero, already indicating a perceptibly wider shock profile in this rarefied flow.

Another research area rewarding the employment of the laser interferometer are unsteady boundary layers. In the shock tube, these are the shock and boundary layer as well as the boundary layer on the rear wall after the reflection of the shock wave. Figure 8 and 9 show the respective arrangement for each signal sample. The thickness for both boundary layers was about 1 mm. The beam separation was kept as small as possible but large enough to ensure that one of the rays was always located outside of the boundary layer. Thus, the density inside the boundary layer was compared to the value outside the boundary layer at every instant in time. To achieve a good spatial resolution, the laser beams were focussed to 0.1 mm diameter within the test section (50 x 50 mm^2). The ray on the near side of the wall was located at a distance of 0.3 mm away from the wall.

In all examples until now, the information is gained from a single time-dependent interference signal, that is, the information from one point in space was considered sufficient. However, there are cases where there is more spatial information necessary for the solution of the problem. For those cases, the laser-interferometer was modified to enable measurements on 8 different image points. A system of additional Wollaston prisms and $\lambda/4$-plates in front of the actual interferometer splits the laser beam into 8 rays. The rays point to several detectors where optical path variations are registered for the respective image points.

In this way, the flow field around a blunt cone was examined. Figure 10 shows a cross section perpendicular to the cone axis and the arrangement of the 8 laser beams. The beams were focussed on a diameter of 0.04 mm at the locus of the cone. The distance between two adjacent rays was only 0.25 mm. The 8 reference beams are as far as possible directed through the undisturbed upstream flow.

Figure 11 shows a series of simultaneously recorded signals. They exhibit time-dependent characteristics typical for the flow generated in a hypersonic shock tube. From every signal, only the constant level during the duration of steady flow has been used for further computations. After several runs with different arrangements, a sufficient number of measurement points were available for the determination of the density profiles.

Figure 12 displays 4 density profiles gained at different cross sections. They were computed applying the Abel inversion of the measured values. This method is applicable only for axisymmetric density distributions, that is, rigorously only for the cone at zero angle of attack. For small angles of attack however, the limited region at the fore of the cone covered by the laser beams can be regarded as approximately radially symmetric. The examined cone was at 10° angle of attack. The density profiles show a marked minimum and thereby indicate an entropy layer from the stagnation region being progressively merged into the boundary layer.

Conclusive Remarks

By citing some examples from shock tube research it has been shown that the laser interferometer described here is an excellent means of diagnosis for gas-dynamic investigations. High resolution in time and space, and high sensitivity in low density (otherwise only achievable with the electron beam absorption method) deserve attention. None of the above examples made full use of the sensitivities feasible. The optical and electronic set-up is relatively simple and easy to operate.

It is safe to assume that the method is applicable to plasma diagnosis as well. For example, a He-Ne laser emitting a wavelength of 3.39 μm in connection with optical parts made of quartz and a suitable IR-detector could be used to determine electron densities. In comparison to the microwave techniques, this method would result in a far better spatial resolution.

Literature

[1] H. Oertel
A Differential Interferometer for Measurements in the Hypersonic Shock Tube.
ISL - Technical Report T 17/61 (1961)

[2] G. Smeets
Differential Interferometer for Observation and Measurement of Boundary Layers.
ISL - Technical Report T 25/64 (1964)

[3] G. Smeets
Differential Interferometer with large ray separation. Data Reduction on the Interferograms.
ISL - Technical Report T 41/68 (1968)

[4] G. Smeets
4-Ray Laser-Interferometer for Measurement of highly transient weak Phase Objects.
ISL - Technical Report T 21/70 (1970)

[5] G. Smeets
Laser-Interferometer for Measurement of highly transient weak Phase Objects.
Opt. Comm. Vol.2 Nr.1 (1970)

[6] G. Smeets
A high-sensitive laser interferometer for transient phase objects.
Shock Tube Research , Proc. 8th, International Shock Tube Symposium (1971)

Appendix with technical details

Light sources

The optical systems described below were set up with two Spectra-Physics He-Ne lasers: Model 132 (1 mW) and Model 124 A (15 mW).

Receivers

In the beginning, photo multipliers were employed:
Philips-Valvo XP 1002 (S 20).

Later on, these were replaced by PIN-diodes from Hewlett Packard, Type 5082-4207. In multi-ray arrangements, PIN-diodes were used in the beginning. Later on, the SA 60 array from United Detector Technology was utilized.

Distances of laser rays in the differential interferometer

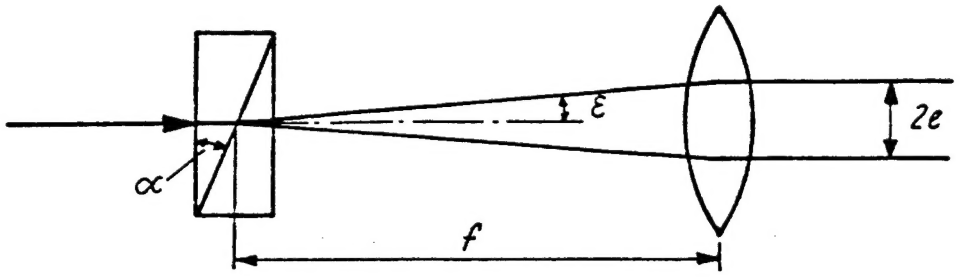

The first Wollaston prism of the differential interferometer splits every light ray (laser beam) into two rays polarized normal to each other. The angle 2ε between the two rays depends on the Wollaston prism angle α, that is:

$$2\varepsilon = 2\tan\alpha \cdot (n_{ex} - n_{or}) .$$

If - as usual - the Wollaston prism is located at the focal point of the main objective with the focal length f, then the distance 2e between the light rays in the test section results from:

$$2e = 2\varepsilon \cdot f = 2f \cdot \tan\alpha \cdot (n_{ex} - n_{or}) .$$

In the following tables, the division angles 2ε and the ray distances 2e are given for some prism angles α and for different focal lengths f (f and 2e in mm).

QUARTZ ($\lambda = 6328$ Å) $(n_{ex} - n_{or}) = 9.05 \cdot 10^{-3}$

α[°]	$2\varepsilon/rd \cdot 10^{-4}$	f=200	250	300	400	500	800	1000	1200	1500	3000
2	6.320	0.1264	0.158	0.189	0.253	0.316	0.505	0.632	0.758	0.947	1.895
4	12.657	0.253	0.316	0.379	0.506	0.632	1.012	1.265	1.518	1.898	3.795
8	25.438	0.509	0.636	0.763	1.017	1.271	2.034	2.543	3.051	3.814	7.629
10	31.916	0.638	0.798	0.957	1.276	1.595	2.553	3.191	3.829	4.786	9.573
20	65.878	1.317	1.646	1.976	2.634	3.293	5.269	6.586	7.904	9.879	19.759
30	104.500	2.090	2.623	3.147	4.196	5.245	8.393	10.491	12.589	15.737	31.473

CALCITE ($\lambda = 6328$ Å) $(n_{or} - n_{ex}) = 0.169$

α[°]	$2\varepsilon/rd \cdot 10^{-4}$	f=200	250	300	400	500	800	1000	1200	1500	3000
2	1.182	2.364	2.965	3.546	4.728	5.910	9.456	11.820	14.184	17.730	35.460
4	2.363	4.726	5.907	7.089	9.452	11.815	18.904	23.63	28.356	35.445	70.891
8	4.752	9.504	11.880	14.256	19.008	23.760	38.016	47.520	57.024	71.280	142.56

Focussing the laser beams in the test section

In order to achieve a spatial resolution as high as possible, the laser beams have to be focussed in the test section. From gaussian theory, the minimal laser ray bundle diameter d_0 in the focal plane and the bundle aperture angle φ are related by:

$$d_0 = \frac{4}{\pi} \cdot \frac{\lambda}{\varphi}.$$

It is assumed that the laser ray bundle intensity distribution is governed by a 2-dimensional gaussian distribution function (TEM_{oo}). d_0 and φ are defined for the point, at which the intensity has dropped to $1/e^2$.

From the constraint, that the ray bundles have to be concentrated on a diameter d over a path length l, it follows geometrically and optically:

$$\varphi \leq \frac{2d}{l}.$$

When substituting $d = d_0$, the smallest diameter, that can be kept over a path length l turns out to be:

$$d = \sqrt{\frac{2}{\pi} \cdot \lambda \cdot l}.$$

To achieve a certain d_0 or φ when setting up an optical arrangement, a simple relation between the bundle diameter D in the first Wollaston prism and the bundle angle φ in the test section is practical:

$$\varphi = \frac{D}{f}.$$

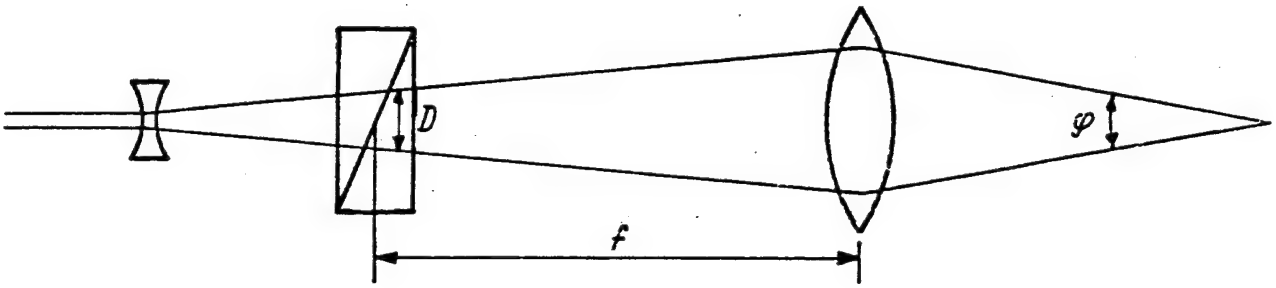

This relationship is independent of the laser beam focal point in the test section.

On the following pages, the optical arrangements, which have been realized until now, are listed. They are specially adapted to fit the widely varying measurement problems.

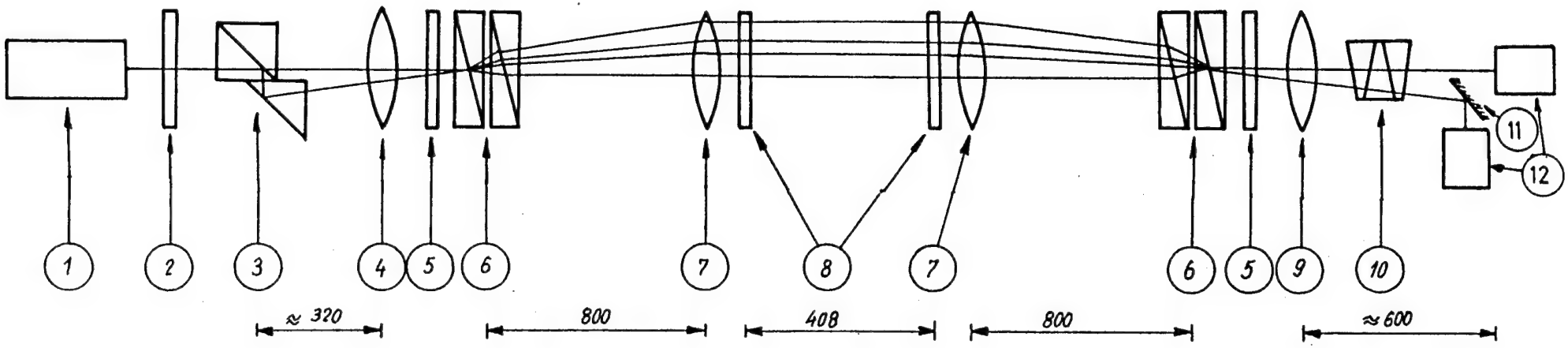

Objective: Density of the Flow and Measurement Time in Shock Tube B

Model: as in Figure 4

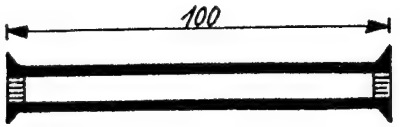

Ray distance 2e = 10.1 mm

Flow Direction

1 Laser (1 mW)
2 Polarization Filter (due to insufficient laser polarization)
3 Beam Splitter
4 Focussing Lens (f = 800 mm)
5 Polarization Filter
6 Wollaston Prisms (2 x 20°)
7 Main Objective Lenses (Doublets, f = 800 mm)
8 Test Section Window
9 Doublet (f = 400 mm)
10 Straight-Sight Prism (was used together with pinholes as a narrow-band filter)
11 Deflection Mirror
12 Photo Multiplier

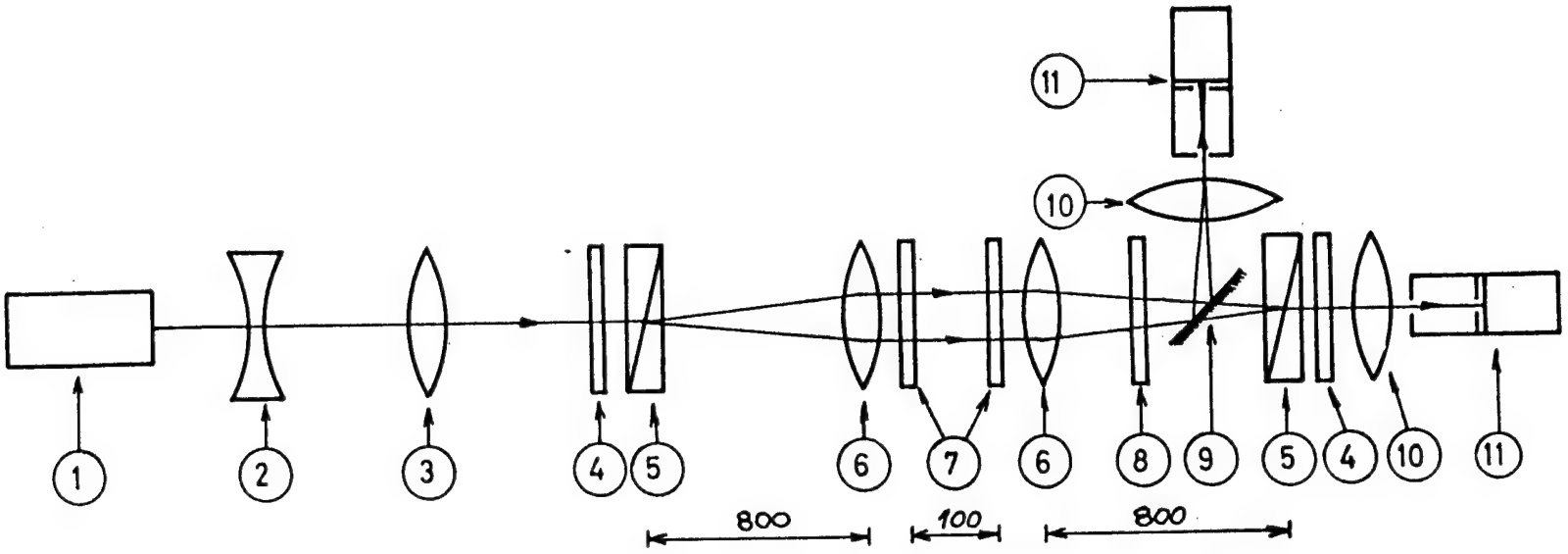

Objective: Observation of the Density Profile in a Shock Tube
Boundary Layer Observation

Model: Rectangular cross section (with and without end plate) without model

Laser beams: 2e = 5.27 mm
d = 0.15 mm
l = 50 mm

1 Laser (1 mW)
2 Lens for beam dispersion (f = -100 mm)
3 Focussing Lens (f = 300 mm)
4 Polarization Filters
5 Wollaston Prisms (20°)
6 Main Objective Lenses (Achromatics, f = 800 mm)
7 Test Section Window
8 Interference Filter
9 Semi-transparent Mirror
10 Objective Lenses (Doublets, f = 400 mm)
11 Photo Multipliers (plus 2 pinholes each)

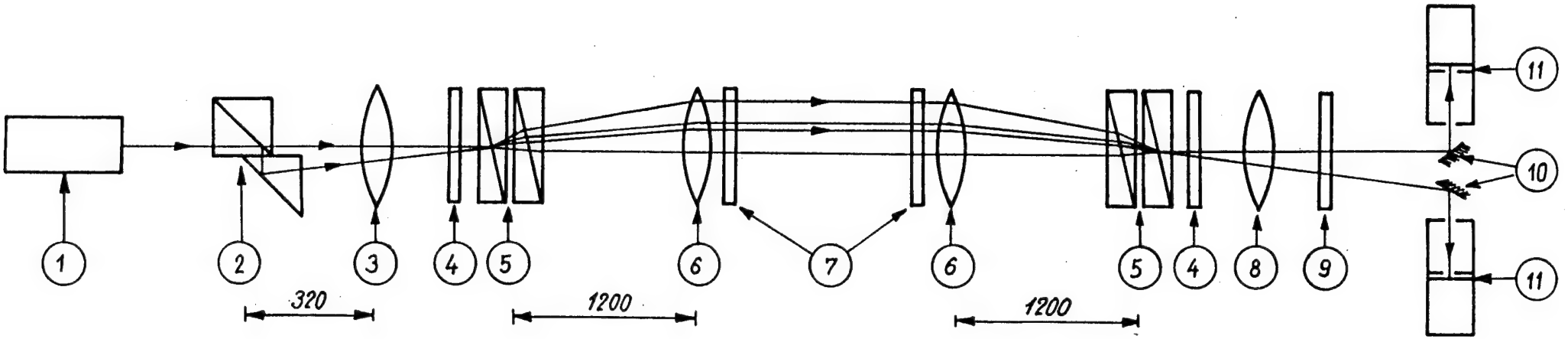

Objective: Density of the Flow and Measurement Time in a Shock Tunnel

Model: as in Figure 4 (length 100 mm)

Ray distance 2e = 15.81 mm

Flow Direction

1 Laser (15 mW)
2 Beam Splitter
3 Focussing Lens (f = 1000 mm)
4 Polarizers
5 Wollaston Prisms (2 x 20°)
6 Main Objective Lenses (f = 1200 mm)
7 Test Section Window
8 Doublet (f = 750 mm)
9 Interference Filter
10 Deflection Mirror
11 Photo Multipliers (plus 2 pinholes each)

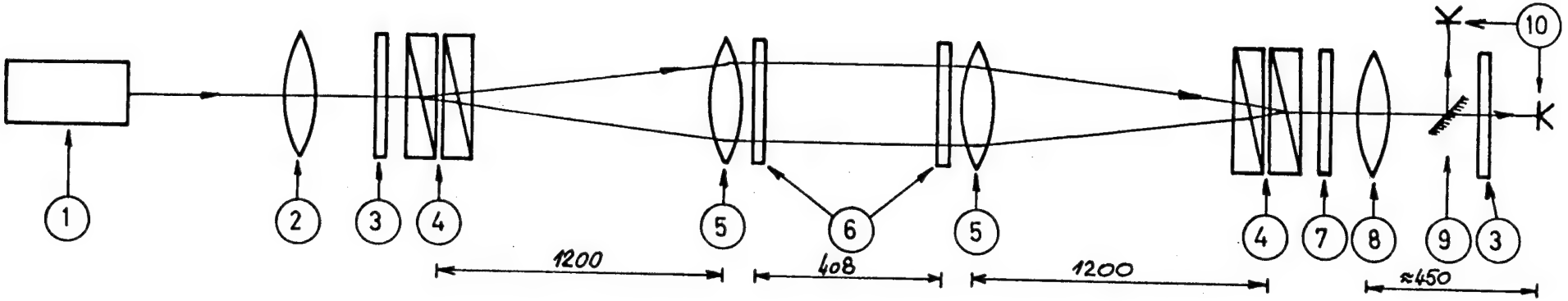

Objective: Density of the Flow and Measurement Time in a Shock Tunnel

Model: as in Figure 4 (length 100 mm)

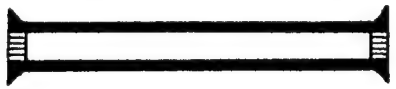

Ray distance 2e = 15.81 mm

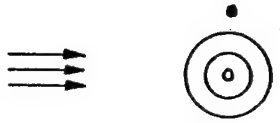

Flow Direction

1 Laser (15 mW)
2 Focussing Lens (f = 1000 mm)
3 Polarizers
4 Wollaston Prisms (2 x 20°)
5 Main Objective Lenses (f = 1200 mm)
6 Test Section Window
7 Interference Filter
8 Objective (f = 135 mm)
9 Deflection Mirror
10 PIN-Diodes

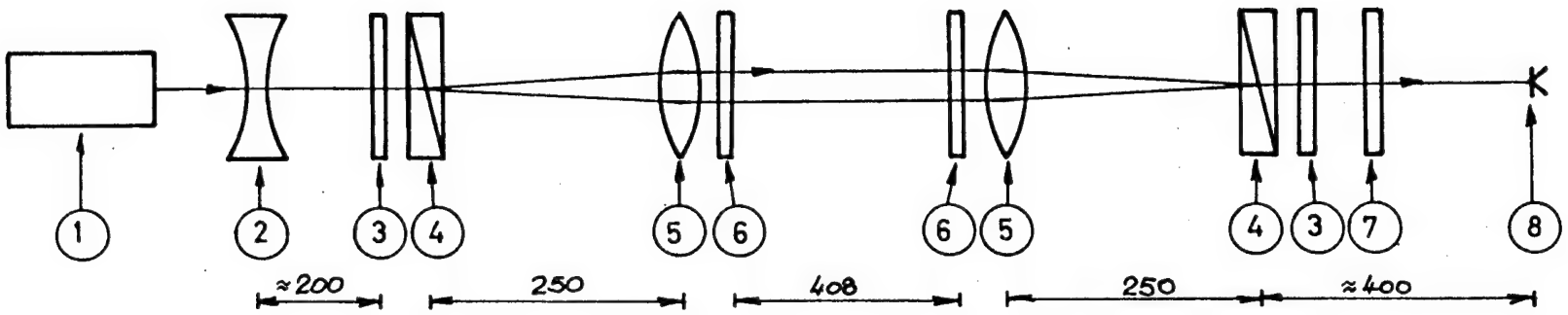

Objective: Calibration Measurement in Heat Transfer
Investigation for Measurement Time Determination

Models: Cones

Laser beams: 2e = 0.79 mm
d = 0.1 mm

1 Laser (1 mW)
2 Dispersion Lens (f = -150 mm)
3 Polarizers
4 Wollaston Prisms (10°)
5 Main Objective Lenses (Doublets, f = 250 mm)
6 Test Section Windows
7 Interference Filter
8 PIN-Diode

Flow Direction

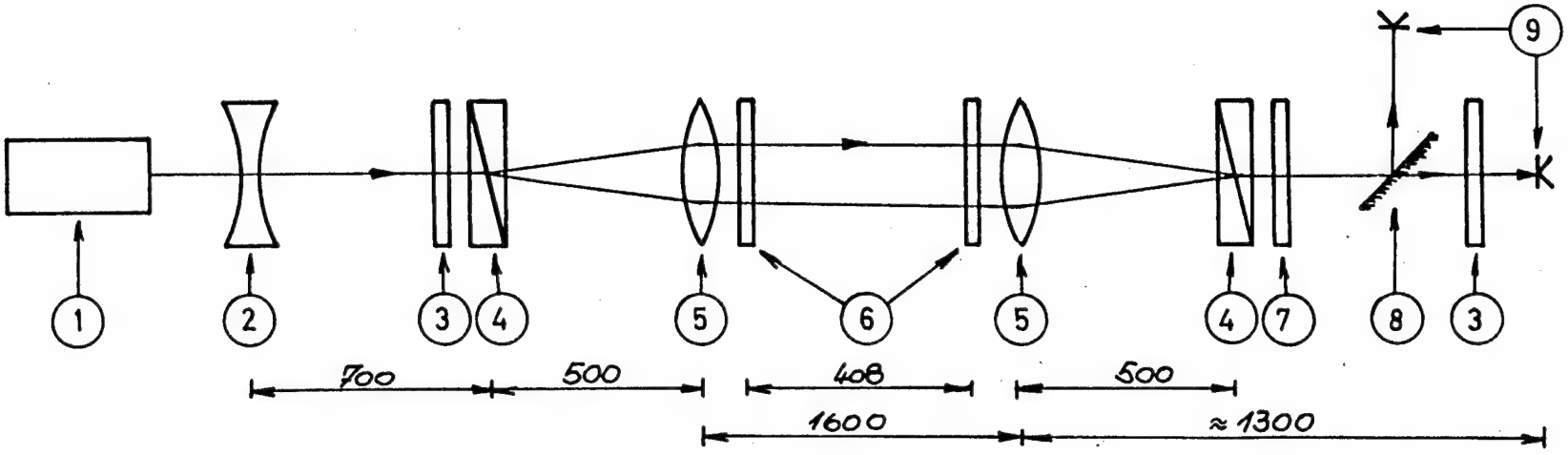

Objective: Entropy and Boundary Layer;
Density Distribution in shock layer around Cone

Models: Cones

Laser beams: 2e = 3.29 mm
d < 0.1 mm

1 Laser (1 mW)
2 Dispersion Lens (f = -100 mm)
3 Polarizers
4 Wollaston Prisms (20°)
5 Main Objective Lenses (Doublets, f = 500 mm)
6 Test Section Window
7 Interference Filter
8 Semi-Transparent Mirror
9 PIN-Diode

Flow Direction

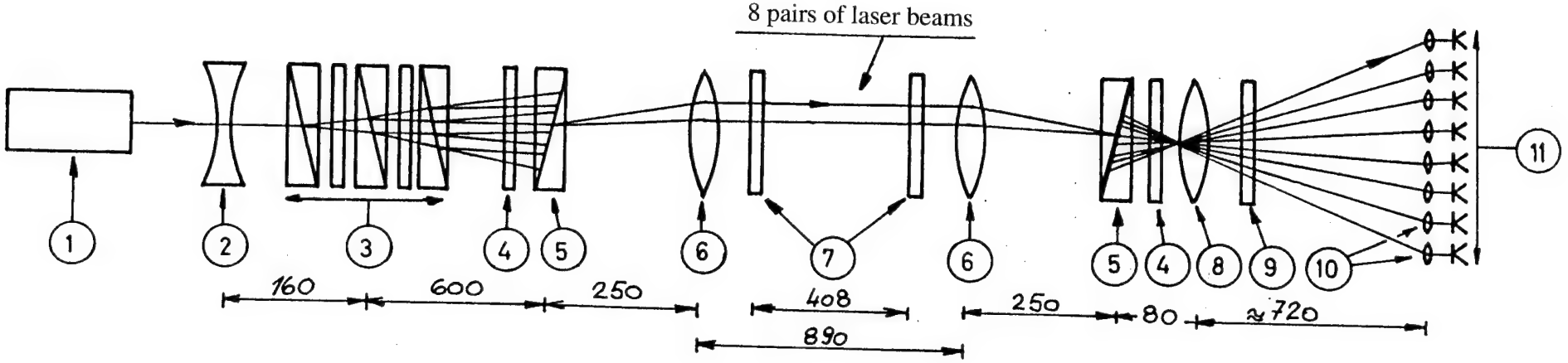

Objective: Entropy and Boundary Layer;
Density Distribution in the Shock Layer around Cone

Models: Cones

Laser beams: 2e = 1.64 mm
d about 0.05 mm

8 ray pairs at 45° to cone axis. Distance between adjacent beams about 0.2 mm.

1 Laser (15 mW)
2 Dispersion Lens (f = -100 mm)
3 Beam Splitter used for generation of 8 beams. Consists of 3 Wollaston prisms of the angles $\alpha = 4°, 8°, 20°$ with polarization filters mounted inbetween
4 Polarizer
5 Wollaston Prisms (20°)
6 Main Objective Lenses (Doublets, f = 250 mm)
7 Test Section Window
8 Objective (microscope objective)
9 Interference Filter
10 Lenses (f = 18 mm)
11 8 PIN-Diodes

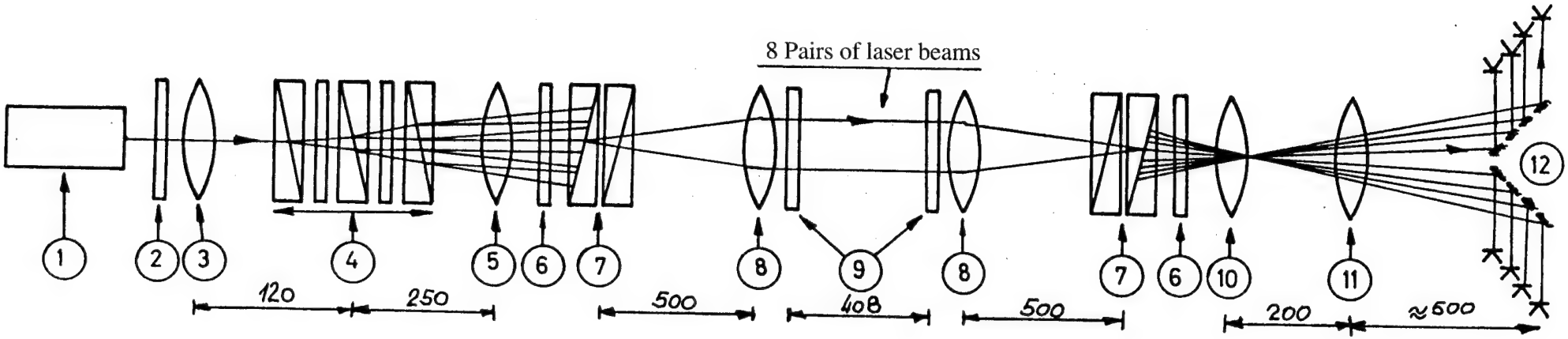

Objective: Entropy and Boundary Layer;
Density Distribution in Shock Layer around Cone

Models: Cones

Laser beams: 2e = 5.24 mm
d about 0.03 mm

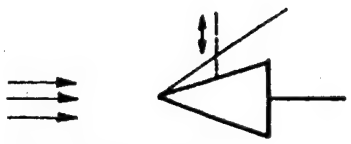

Flow Direction

8 ray pairs at 45° to cone axis. Distance between adjacent beams about 0.2 mm.

1 Laser (15 mW)
2 λ/4-Plate
3 Dispersion Lens (f = 30 mm)
4 Beam Splitter used for generation of 8 beams. Consists of 3 Wollaston prisms of the angles $\alpha = 4°, 8°, 20°$ with λ/4-plates mounted inbetween
5 Focussing Lens (f = 300 mm)
6 Polarization Filter
7 Wollaston Prisms (20° + 10°)
8 Main Objective Lenses (Doublets, f = 500 mm)
9 Test Section Window
10 Objective (f = 90 mm)
11 Microscope Objective (f = 5 mm)
12 Detector Unit (contains 8 small mirrors and 8 PIN-diodes)

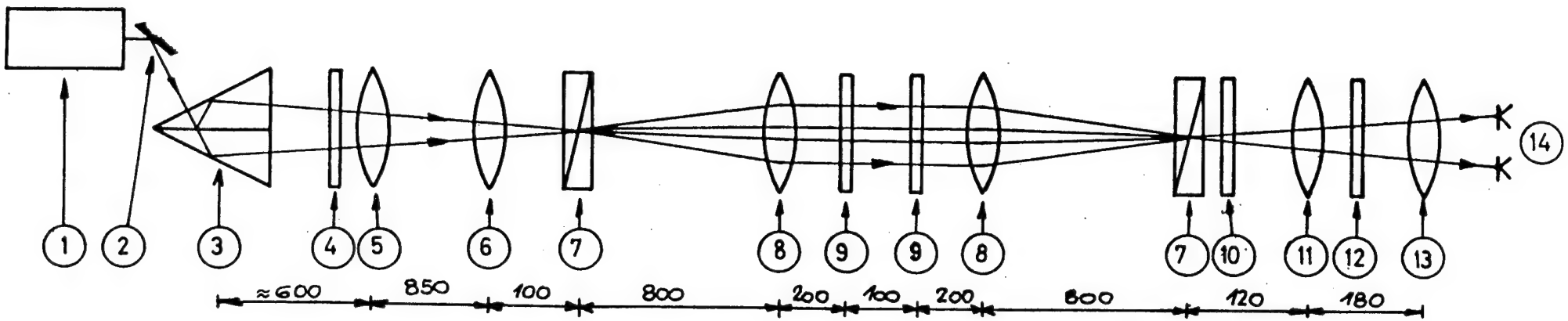

Objective: Shock Wave Density Profile

Models: 3 Capillaries of different lengths

Laser beams: 2e = 5.27 mm
d about 0.1 mm

Flow Direction

1 Laser (15 mW)
2 Deflecting Mirror
3 Koester Prism
4 λ/4-Plate
5 Dispersion Lens (f = 40 mm)
6 Focussing Lens (f = 200 mm)
7 Wollaston Prisms (20°)
8 Main Objective Lenses (Doublets, f = 800 mm)
9 Test Section Window
10 Polarization Filter
11 Objective (Doublet, f = 180 mm)
12 Interference Filter
13 Objective (Doublet, f = 200 mm)
14 PIN-Diodes

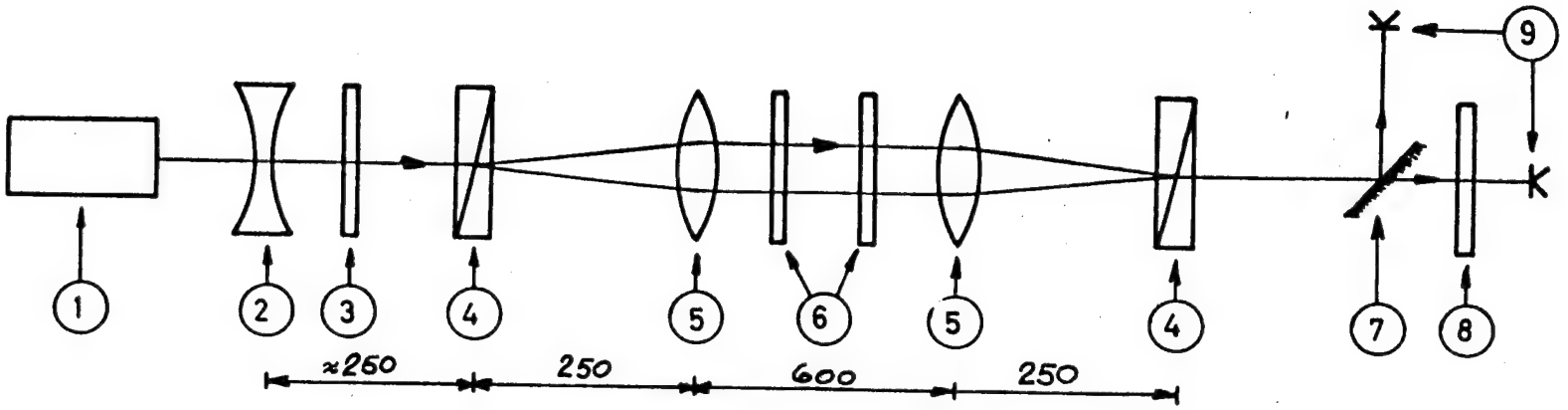

Objective: Bow Shock of a small sphere

Models: Ball (Dia. = 2 mm)

Laser beams: 2e = 0.79 mm
d about 0.05 mm

1 Laser (15 mW)
2 Dispersion Lens (f =-60 mm)
3 λ/4-Plate
4 Wollaston Prisms (10°)
5 Main Objective Lenses (Doublets, f = 250 mm)
6 Test Section Window
7 Semi-Transparent Mirror
8 Polarization Filter
9 PIN-diodes

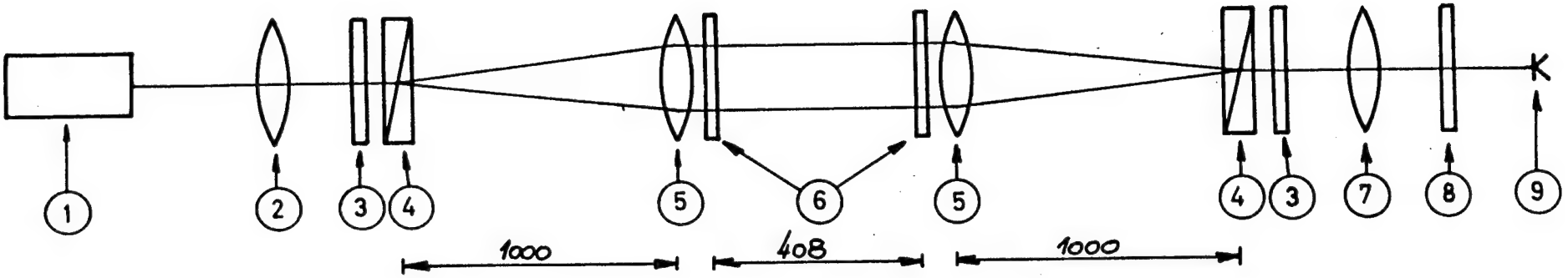

Objective: Test for Steady Flow Regime

Models: Cone with Cockpit

Laser beams: 2e = 10.49 mm

1 Laser (1 mW)
2 Focussing Lens (f =-1000 mm)
3 Polarization Filter
4 Wollaston Prisms (30°)
5 Main Objective Lenses (Achromatics, f = 1000 mm)
6 Test Section Window
7 Achromatic (f = 200 mm)
8 Interference Filter
9 PIN-diode

Flow Direction

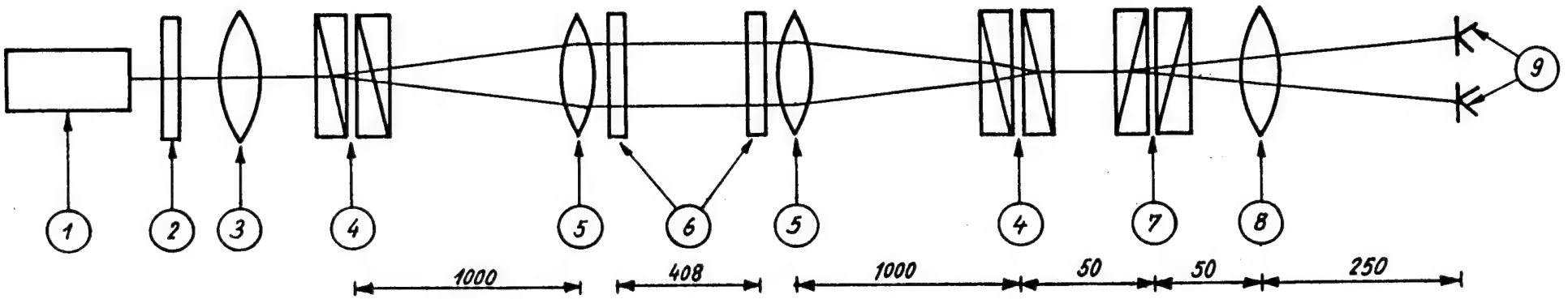

Objective: Density of the Flow and Measurement Time in a Shock Tunnel

Model: as in Figure 4

Ray distance 2e = 16.71 mm

FlowDirection

1 Laser (15 mW)
2 λ/4-Plate
3 Dispersion Lens (f = 1000 mm)
4 Wollaston Prisms (20° + 30°)
5 Main Objective Lenses (Doublets, f = 1000 mm)
6 Test Section Window
7 Wollaston Prisms (20° + 30°) for generation of two complementary-phased interference signals
8 Objective (f = 250 mm)
9 2 PIN-Diodes

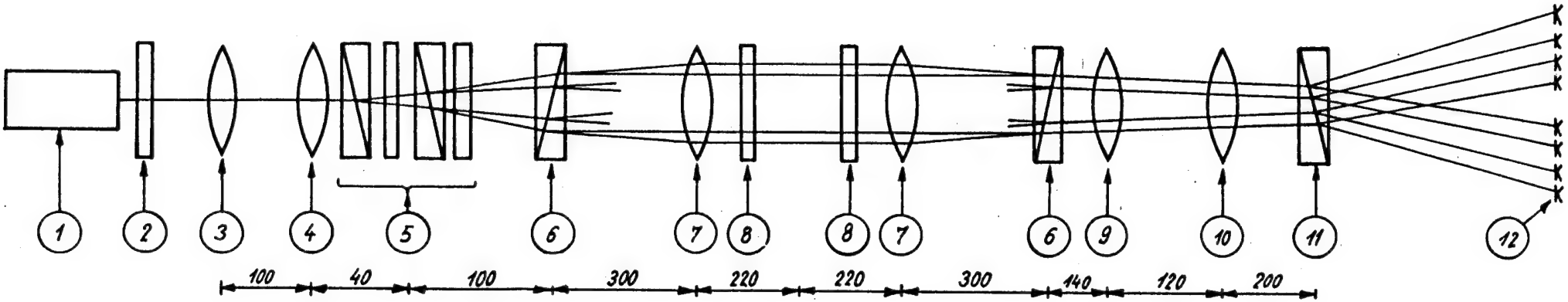

Objective: Laminar Boundary Layer

Model: Tube Dia. 30 mm, parallel to shock tube axis

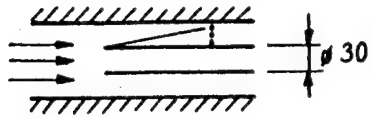

Laser beams: 2e = 1.98 mm
d about 0.05 mm

4 ray pairs at 90° to the flow direction. Distance between adjacent rays 0.22 mm.

1 Laser (15 mW)
2 λ/4-Plate
3 Dispersion Lens (Doublet, f = 20 mm)
4 Objective for Focussing (Doublet, f = 100 mm)
5 Beam Splitter for Generation of 4 beams, consisting of 2 Wollaston prisms of angles 2° and 4° with λ/4-plate and polarization filter
6 Wollaston Prisms (20°)
7 Main Objective Lenses (Doublets, f = 300 mm)
8 Test Section Window
9 Objective (f = 105 mm)
10 Microscope Objective (f = 5 mm)
11 Wollaston Prisms (8°) of Calcite for generation of two complementary-phased interference signals

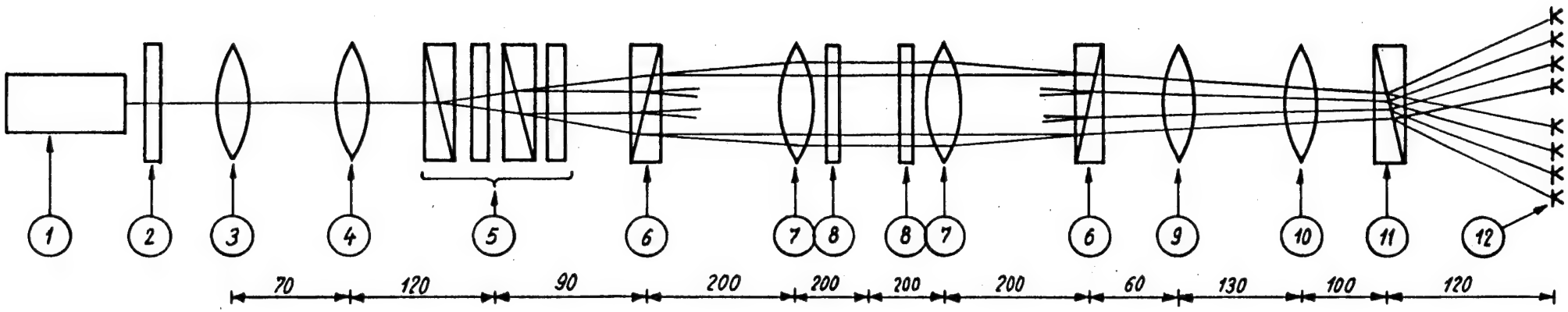

Objective: Turbulent Boundary Layer

Model: Tube Dia. 30 mm, parallel to shock tube axis

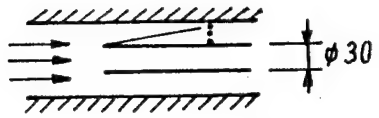

Laser beams: 2e = 0.126 mm
d about 0.01 mm

4 ray pairs at 90° to the flow direction. Distance between adjacent rays 0.126 mm.

1 Laser (15 mW)
2 λ/4-Plate
3 Dispersion Lens (Doublet, f = 10 mm)
4 Objective for Focussing (Doublet, f = 90 mm)
5 Beam Splitter for Generation of 4 beams, consisting of 2 Wollaston prisms of angles 10° and 20° with λ/4-plate and polarization filter
6 Wollaston Prisms (2°)
7 Main Objective Lenses (Doublet, f = 200 mm)
8 Test Section Windows
9 Objective (f = 105 mm)
10 Objective (f = 20 mm)
11 Wollaston Prisms (8°) of Calcite for generation of two complementary-phased interference signals
12 Multiple Detector (UDT PIN-SA 60)

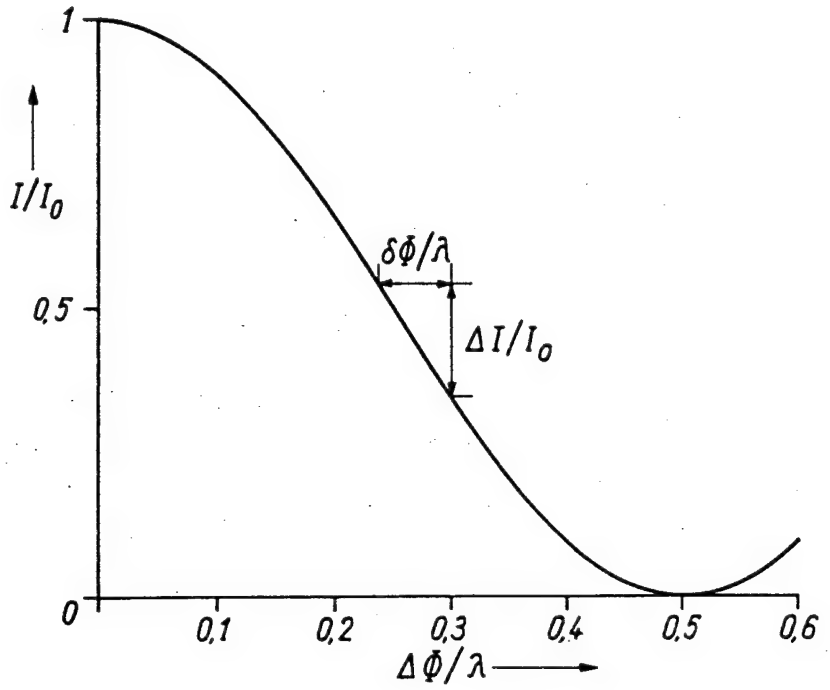

Fig. 1 - Relationship between Optical Path Variation δϕ and Intensity Variation ΔI

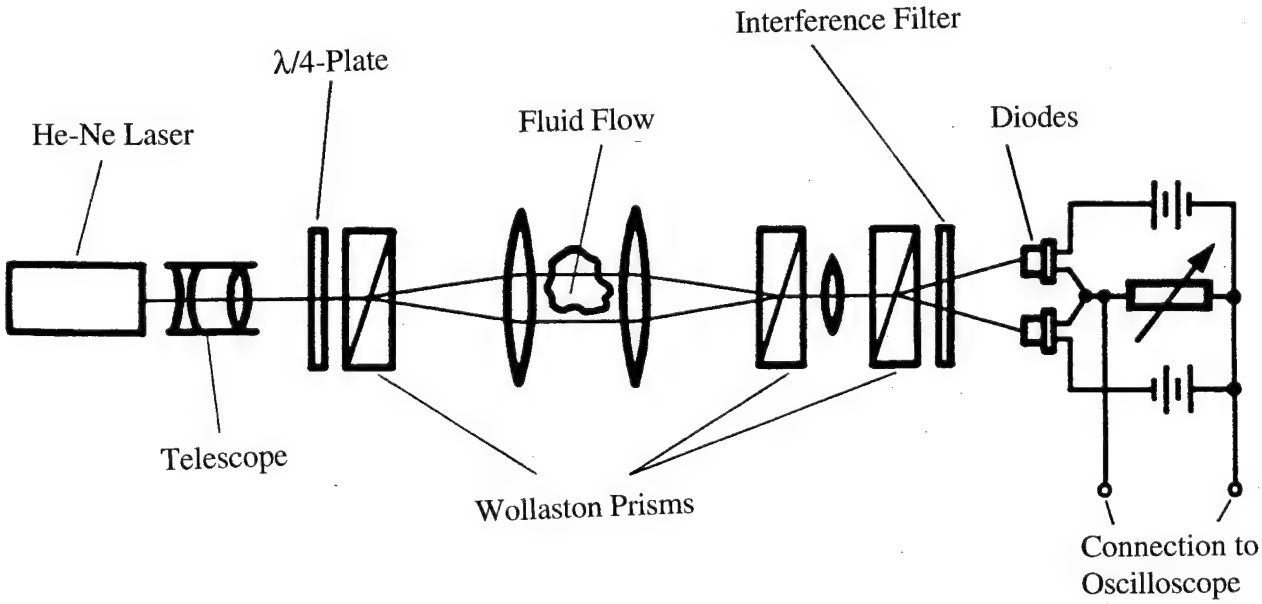

Fig. 2 - Laser-Interferometer

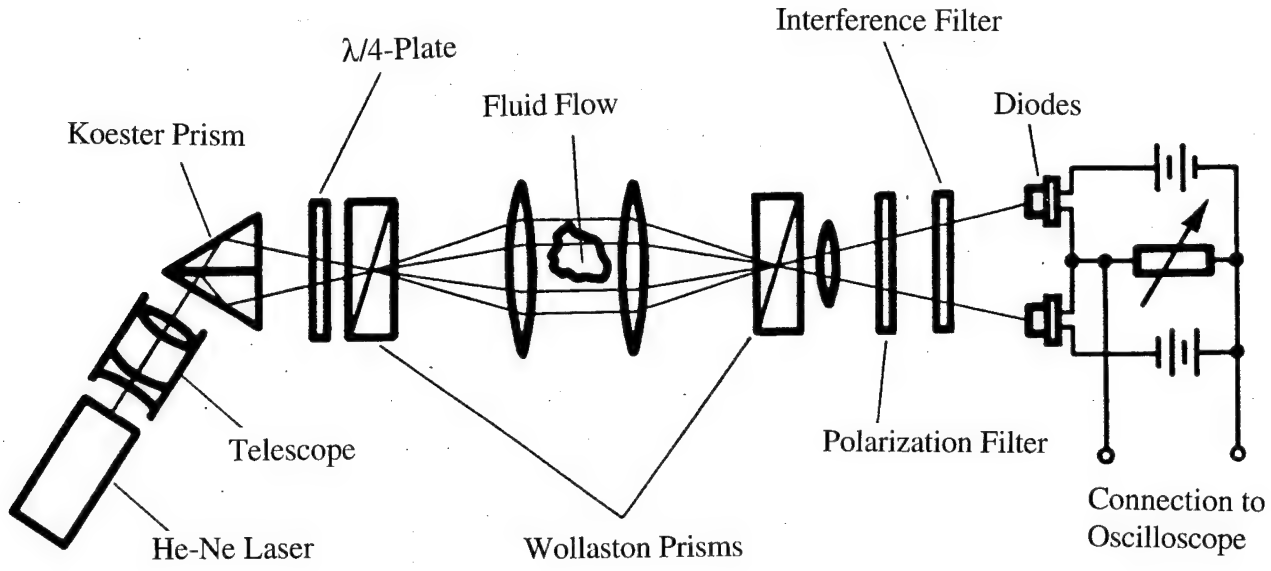

Fig. 3 - Laser-Interferometer (with Compensation of Sensitivity to Vibrations)

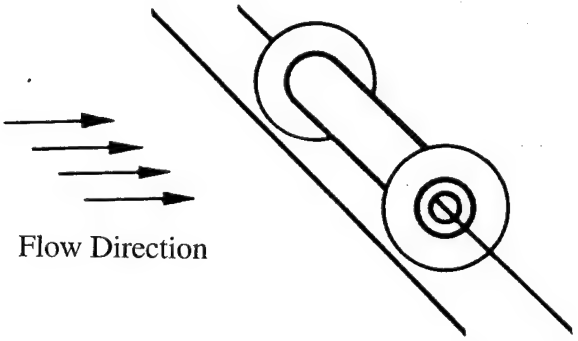

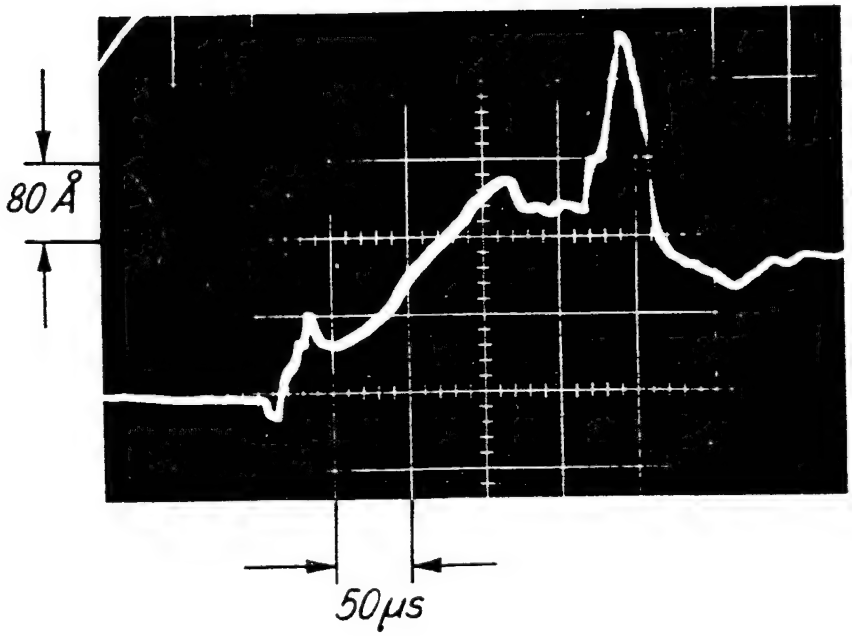

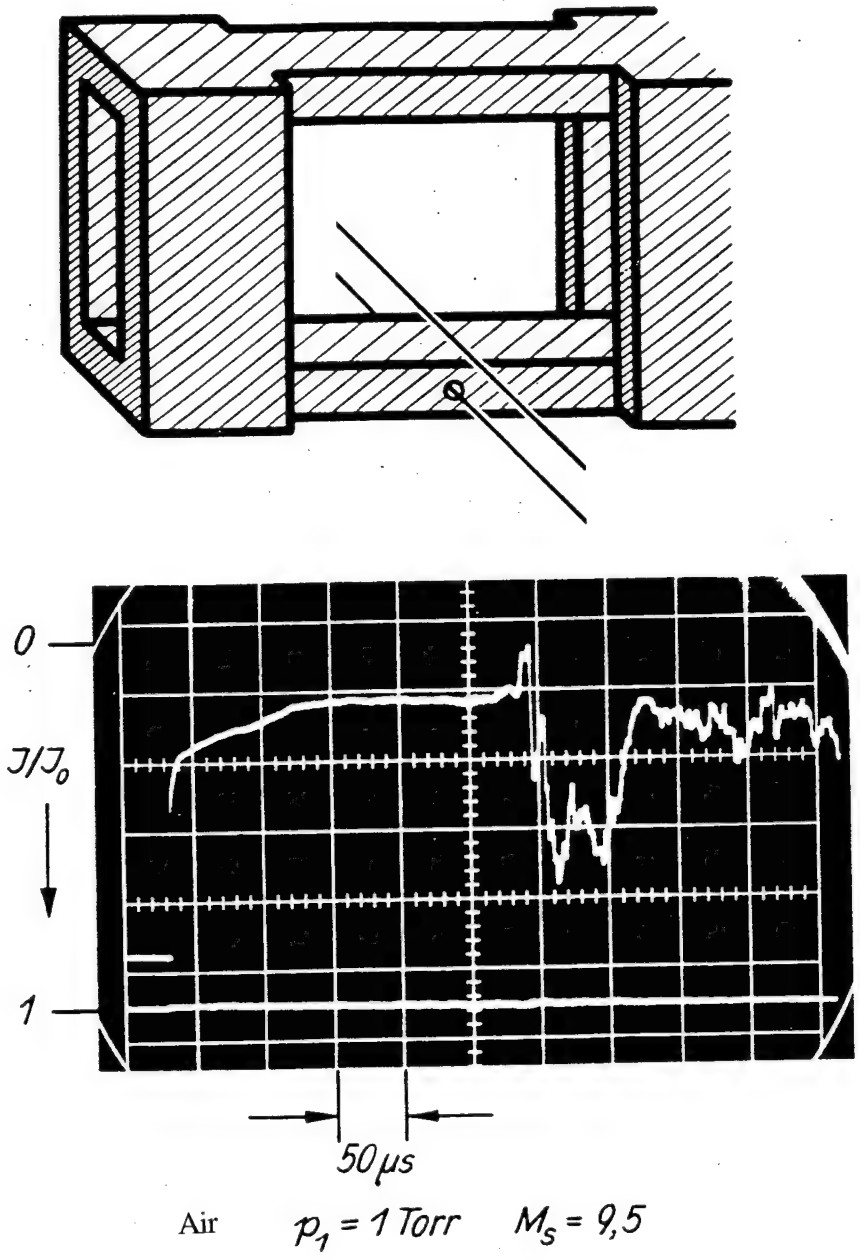

Fig. 5 - Measurement of Density Profile in the Shock Tube

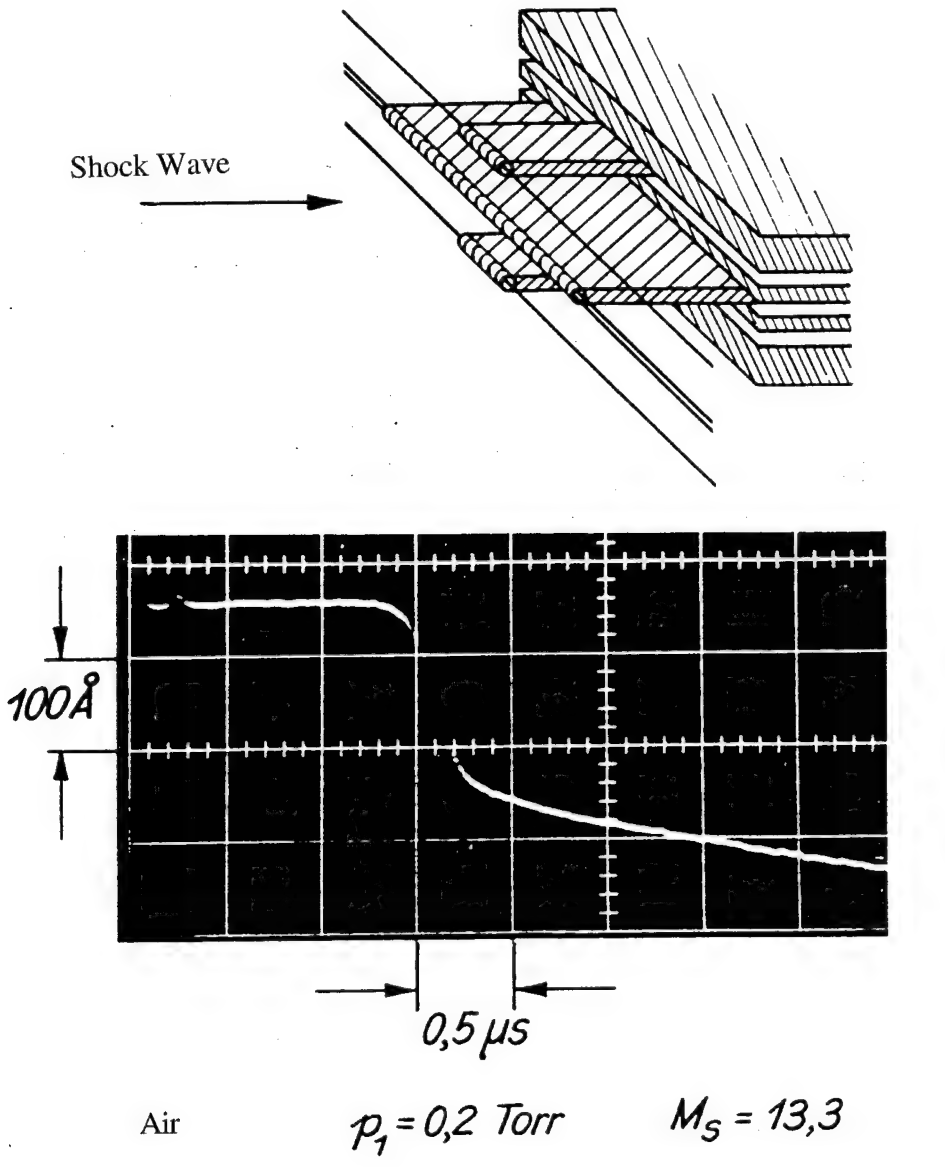

Fig. 6 - Density Profile Measurement within a Shock Front

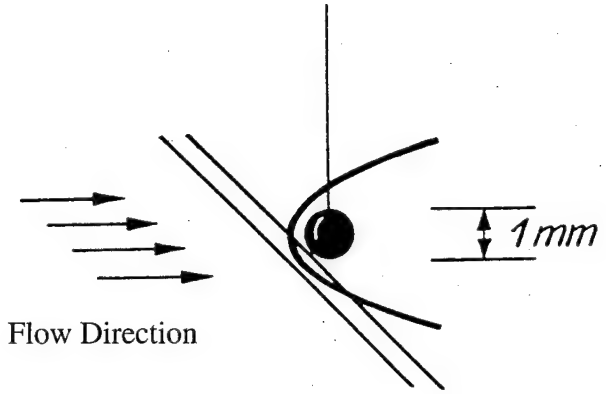

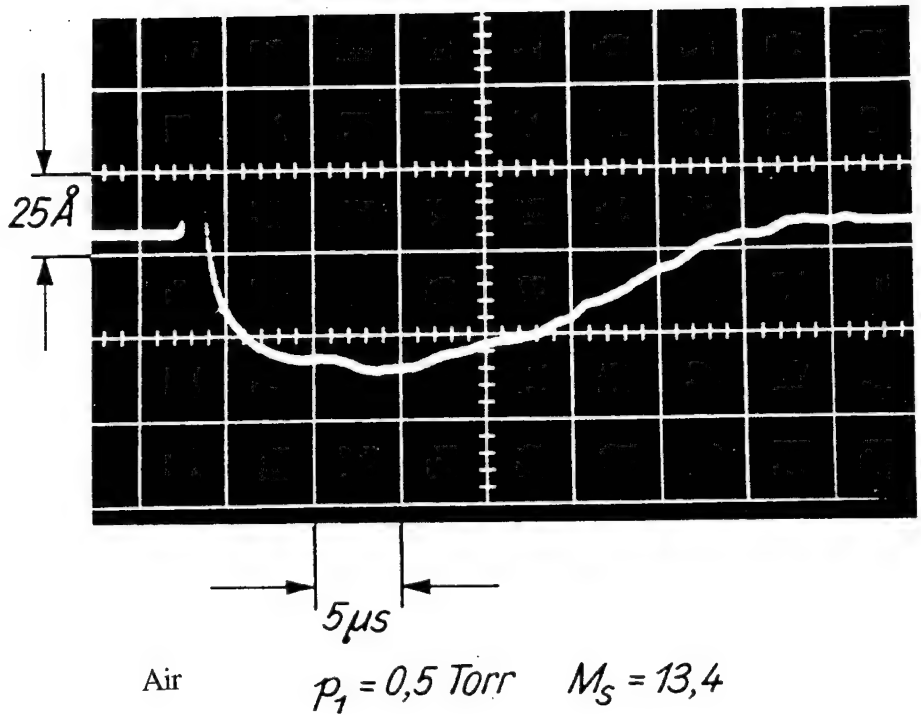

Fig. 7 - Investigation of the Stagnation Region of a Small Sphere

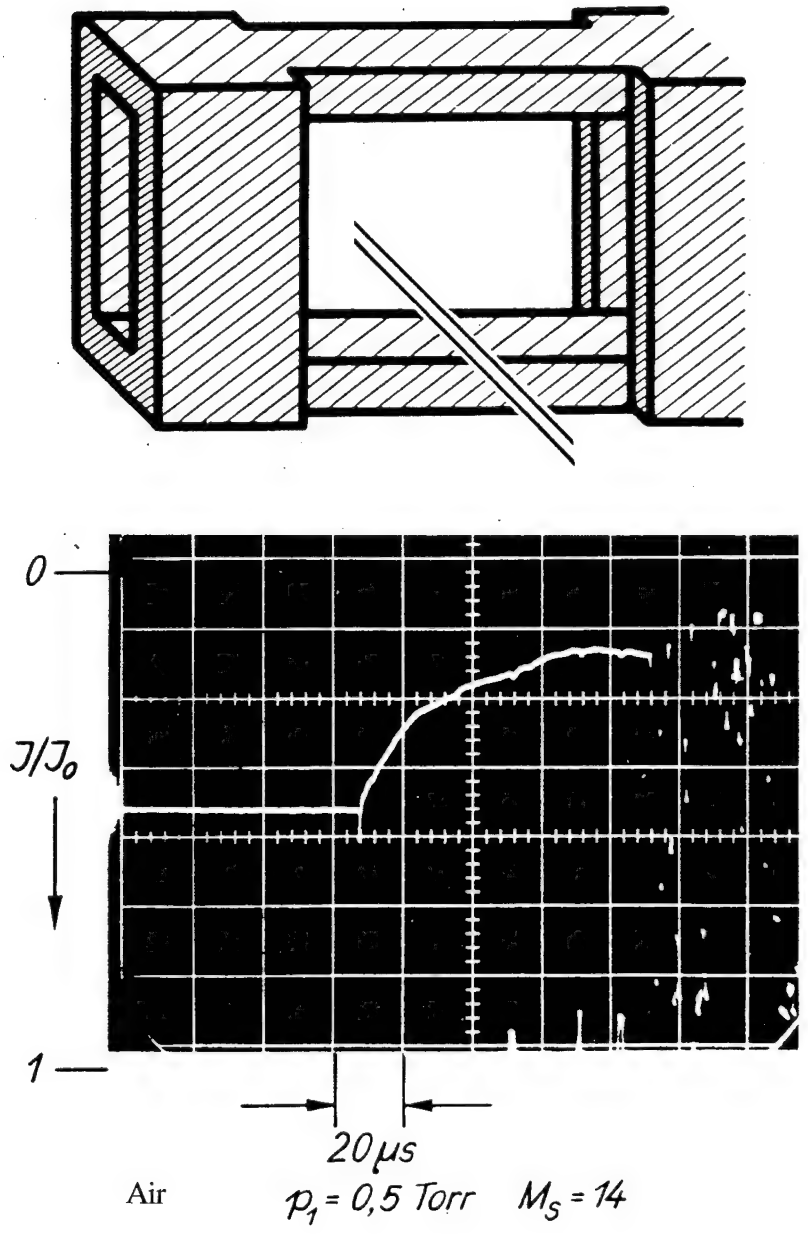

Fig. 8 - Recording of Unsteady Shock Wave Boundary Layer

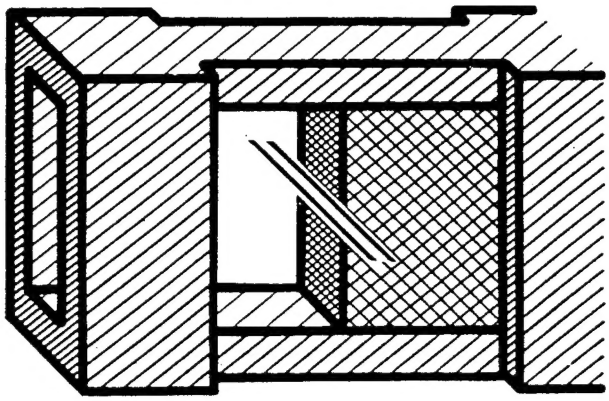

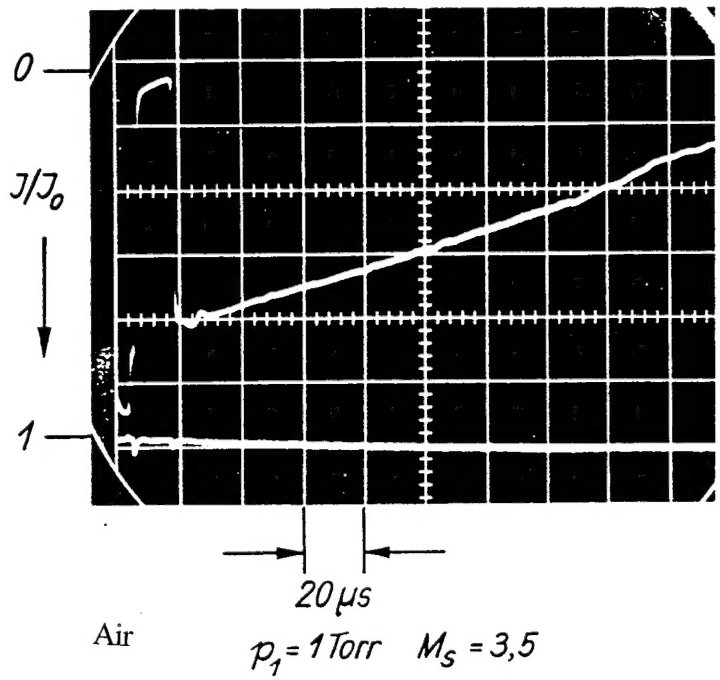

Fig. 9 - Recording of Thermal Boundary Layer at the End Plate of a Shock Tube

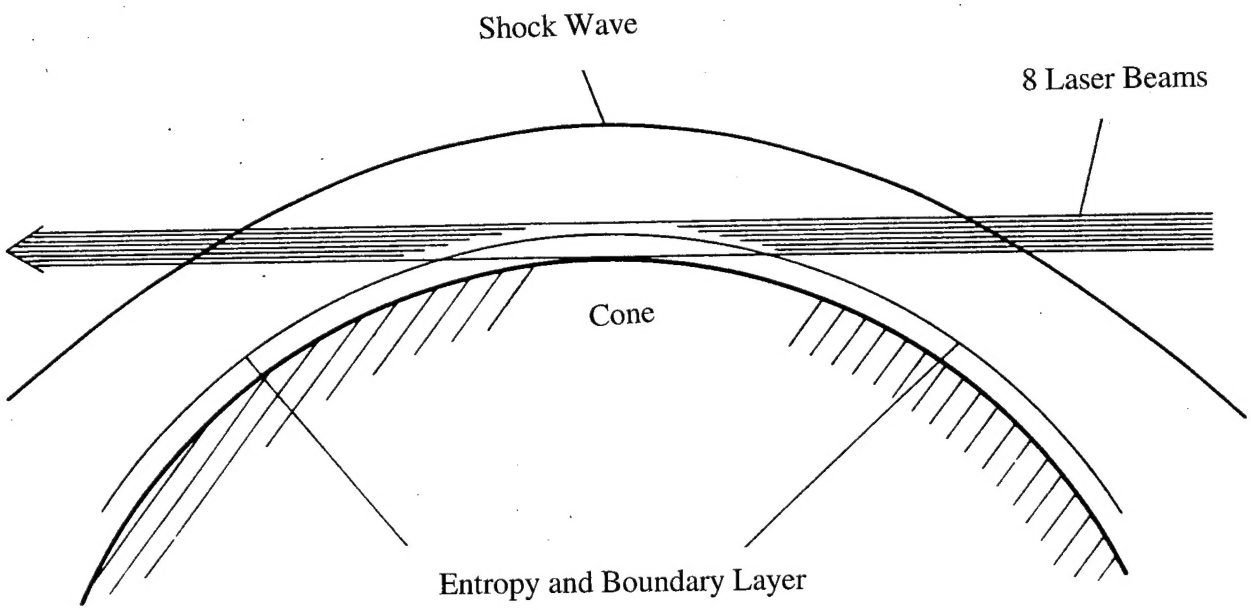

Fig. 10 - Laser Beam Arrangement for Determination of the Flow around a Cone

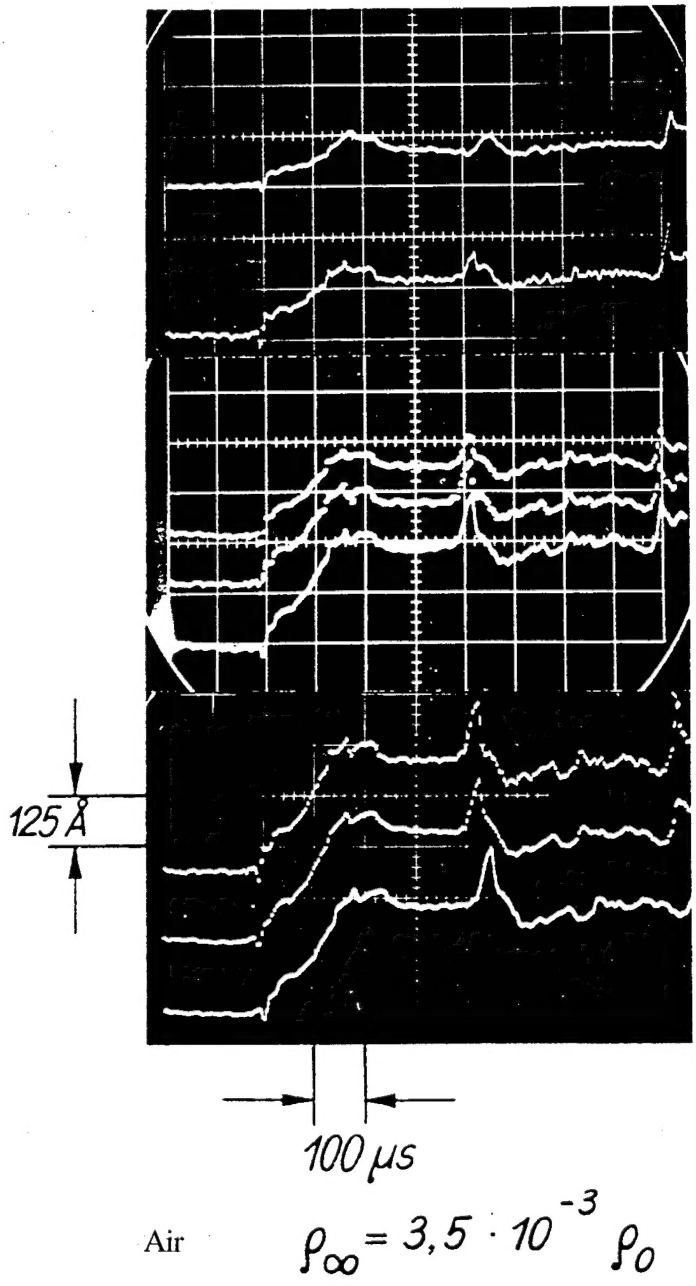

Fig. 11 - Series of Simultaneous Signals from Cone Flow

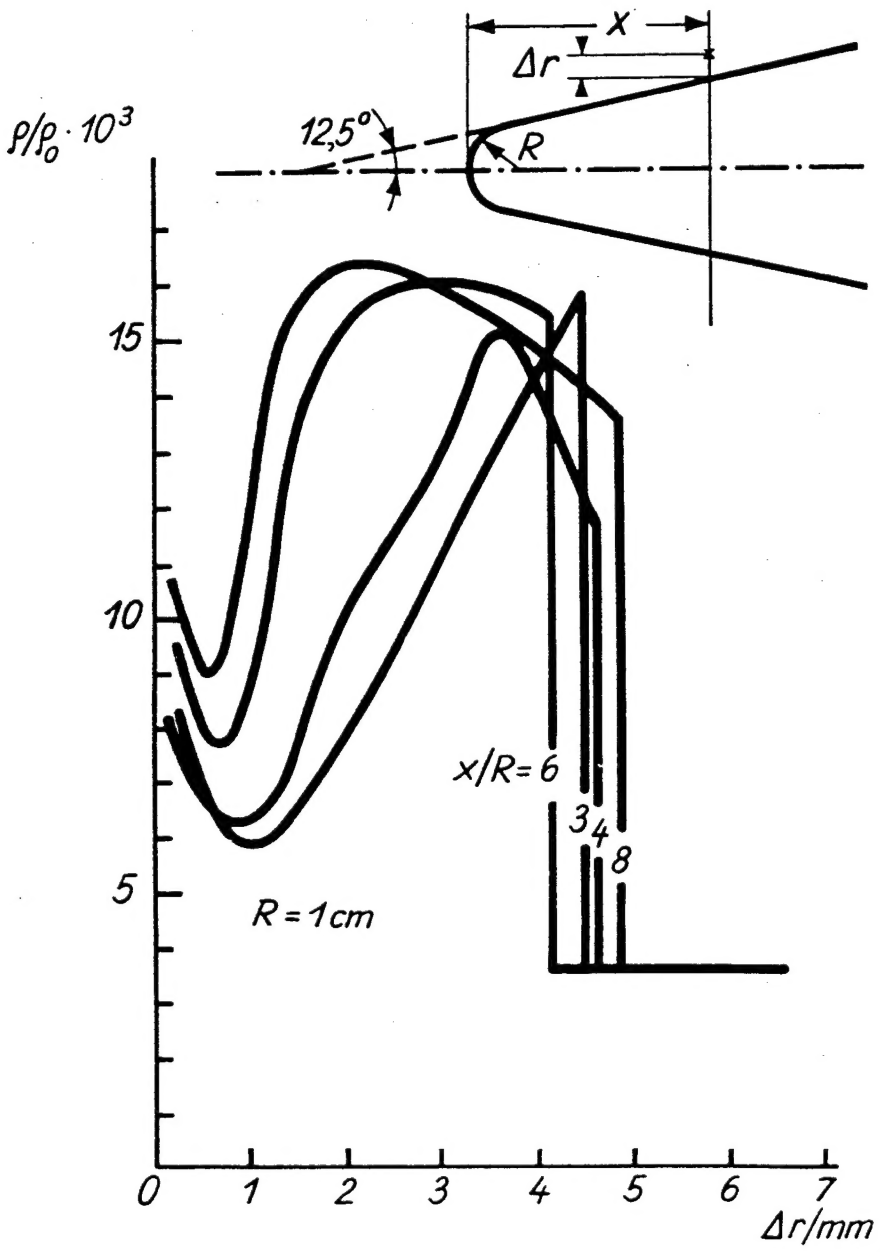

Fig. 12 - Density Profiles at different Locations within the Shock Layer of A Cone